

# Measurements of the Charm Charge Separation and Constraints for Lighter Quark Flavours

Andrew Halley (MPI München)<sup>1</sup>    Pascal Perrodo (CERN)

February 8, 1995

## Abstract

Two complimentary measurements of the mean hemisphere charge for  $c$  quarks are presented. Their results are combined, taking into account fully the correlations between methods and data samples, to yield a relative precision of better than 9%. The results from data are then compared with model expectations in the light of recently updated measurements of charm branching fractions. Constraints on separations for light quark, ( $u, d, s$ ), flavours are also calculated and compared with hadronisation models.

## 1 Introduction

Recent ALEPH measurements of electroweak asymmetries [1, 2, 3] and  $B^0\bar{B}^0$  mixing [4] make use of the charm quark's charge separation,  $\delta_c$ . This quantity is defined to be the charge difference between hemispheres in  $c\bar{c}$  events. The hemisphere charges are calculated using a sum over the particle charges, weighted by their longitudinal momenta relative to a given event axis. Until recently asymmetry and mixing measurements had to depend on Monte Carlo estimates for the value of  $\delta_c$ . The validity of such estimates has recently been brought into question by a comprehensive study of the JETSET<sup>2</sup> model's [5] expectations [6]. This indicates inconsistencies between recently measured inclusive rates of  $D$  decays and those used previously. The value of these decay rates affect  $\delta_c$  quite considerably and their experimental uncertainties give rise to large systematic errors which are unlikely to improve dramatically in the near future.

Consequently, it is of interest to extract  $\delta_c$  from ALEPH data as far as possible, so that it does not limit current and future precision measurements. This is rather difficult experimentally due to problems of selecting a large  $c\bar{c}$  sample and determining the orientation of the  $c\bar{c}$  pair prior to fragmentation.

Two different approaches are presented here. In the first, hemispheres containing a fast  $D^{*\pm}$  are selected to obtain an enriched  $c\bar{c}$  sample. The hemisphere charge on the other side is then signed opposite to that of the meson candidate. The second method uses a lifetime tag to isolate an inclusive sample of  $c\bar{c}$  and  $b\bar{b}$  events and compares the two hemisphere charges in each event to determine the mean  $\delta_c$  and  $\delta_b$  from a simultaneous fit. For the purposes of comparison, both methods calculate the hemisphere charge using longitudinal momentum weights relative to the thrust axis which is determined using the ENFLW objects. The results when only charged tracks are used are compatible and are given in the Appendix.

The two methods are largely independent and are described separately in Sections 2 and 3. Extracting the combined set of  $\delta_c$  values for a range of the weighting power,  $\kappa$ , involves common assumptions and correlations which are discussed in Section 4. The combined results are then given and discussed in Section 5.

## 2 A Measurement of $\delta_c$ Using a $D^{*\pm}$ Tag

This method is based upon a preliminary measurement outlined in [6]. The technique is now fully advanced and a complete description and set of results are given here. The principle of the

---

<sup>1</sup>Now at the University of Glasgow, Scotland, United Kingdom.

<sup>2</sup>In the context of the HVFL03 generator.

Decay mode	Candidates	Background
$D^0 \rightarrow K\pi$	1071	$46 \pm 33$
$D^0 \rightarrow K\pi\pi\pi$	4197	$1930 \pm 70$
$D^0 \rightarrow K\pi\pi^0$	3940	$1500 \pm 73$

Table 1: Number of candidates events for the three  $D^0$  channels, together with their estimated backgrounds.

method is to select events based on the presence of a high momentum  $D^{*\pm}$  in one hemisphere. The charge of the  $D^{*\pm}$  is used to sign the hemisphere charge measured in the opposite half of the event.  $\langle Q_{opp} \rangle$ . This yields a sample, predominantly consisting of  $c\bar{c}$  events, with a significant  $b\bar{b}$  and much smaller light quark contamination.  $\delta_c$  is extracted by :

- Correcting for backgrounds to the true  $D^{*\pm}$  signal from light quark and combinatoric events.
- Correcting for any bias to the hemisphere charge from the selection of  $D^{*\pm}$  candidates in the opposite hemisphere.
- Correcting for the remaining  $b\bar{b}$  contribution from  $b \rightarrow c \rightarrow D^{*+}$  and  $b \rightarrow W \rightarrow D^{*-}$  events.

The selection of  $D^{*\pm}$  samples in ALEPH is explained in detail in [7]. Three decay modes are searched for. The samples found are shown in Table 1 and are based on 1990  $\rightarrow$  1993 data. A corresponding side-band sample is selected for each sample of candidates. After background subtraction using the side-bands, the charm fraction in the remaining sample is estimated to be [8] :

$$f_c = 79 (\pm 3) \% \quad (1)$$

The fraction is found to be independent of the selected decay mode within the quoted experimental uncertainty. The measured values of  $\langle Q_{opp} \rangle$  are given in Table 2 and may be considered as composed of four components from  $c\bar{c}$ ,  $b\bar{b}$ , light quark and combinatoric events. The effects of these are discussed separately as different methods are required to account for each component.

## 2.1 Corrections for Light Quark and Combinatoric Backgrounds

Light quark and combinatoric events are most simply removed by subtracting the value of  $\langle Q_{opp} \rangle$  obtained in side bands,  $\langle Q_{opp}^{side} \rangle$ , obtained from the  $D^{*\pm}$  selection in data. The flavour composition of the side-bands depends on the  $D^{*\pm}$  decay selected and so  $\langle Q_{opp}^{side} \rangle$  is extracted from the data for each mode. The mean hemisphere charges, corrected for light quark and combinatoric events, is then :

$$\langle Q_{opp}^{D^*} \rangle = \langle Q_{opp} \rangle - (1 - f_{D^*}) \langle Q_{opp}^{side} \rangle \quad (2)$$

where  $\langle Q_{opp}^{D^*} \rangle$  is the hemisphere charge opposite true  $D^{*\pm}$  rather than simply that opposite  $D^{*\pm}$  candidates and  $f_{D^*}$  is the fraction of candidates which are in fact true  $D^{*\pm}$ . The latter is obtained by extrapolating and integrating the sidebands underneath  $D^{*\pm}$  peak in the mass spectrum. The values of  $\langle Q_{opp}^{D^*} \rangle$  are given in Table 3 for the three selected decay modes. The side-band charges are compatible with zero for all decay modes and values of the charge weighting power,  $\kappa$ . In addition, the values of  $\langle Q_{opp}^{D^*} \rangle$  are also compatible with each other for all decays modes and  $\kappa$ .

$\kappa$	$\langle Q_{opp} \rangle (K\pi)$	$\langle Q_{opp} \rangle (K\pi\pi\pi)$	$\langle Q_{opp} \rangle (K\pi\pi^0)$
0.3	$0.0638 \pm 0.0055$	$0.0368 \pm 0.0032$	$0.0401 \pm 0.0034$
0.4	$0.0644 \pm 0.0060$	$0.0362 \pm 0.0035$	$0.0409 \pm 0.0037$
0.5	$0.0646 \pm 0.0066$	$0.0354 \pm 0.0039$	$0.0416 \pm 0.0041$
0.7	$0.0642 \pm 0.0081$	$0.0334 \pm 0.0047$	$0.0425 \pm 0.0049$
0.9	$0.0631 \pm 0.0098$	$0.0313 \pm 0.0056$	$0.0427 \pm 0.0058$
1.0	$0.0625 \pm 0.0106$	$0.0303 \pm 0.0061$	$0.0426 \pm 0.0063$
1.2	$0.0611 \pm 0.0121$	$0.0285 \pm 0.0069$	$0.0421 \pm 0.0071$
1.5	$0.0591 \pm 0.0141$	$0.0266 \pm 0.0080$	$0.0408 \pm 0.0082$
2.0	$0.0567 \pm 0.0167$	$0.0254 \pm 0.0094$	$0.0381 \pm 0.0097$
$\infty$	$.0508 \pm .0197$	$0.0203 \pm 0.0102$	$0.0321 \pm 0.0122$

Table 2: Measured Values of  $\langle Q_{opp} \rangle$  for the three selected  $D^{*\pm}$  modes.

## 2.2 Corrections for Selection Bias and $b$ Quarks

The measurement of  $\langle Q_{opp}^{D^*} \rangle$  contains contributions from  $c\bar{c}$  and  $b\bar{b}$  events which may be written as :

$$\langle Q_{opp}^{D^*} \rangle = \frac{1}{2} [f_c (\delta_c + \epsilon_c) + (1 - f_c) (\delta_b + \epsilon_b)] \quad (3)$$

where  $f_c$  is the  $c\bar{c}$  fraction given in (1) and  $(\epsilon_c, \epsilon_b)$  are correction factors to take into account any bias the  $D^{*\pm}$  selection may have on  $(\delta_c, \delta_b)$ . There are two sources of such bias :

- The presence of a fast, high-mass state such as the  $D^{*\pm}$  in one hemisphere improves the determination of the thrust axis. This is used to calculate the weights given to particle charges in the hemisphere charge calculation and leads to an increase in the values of  $(\delta_c, \delta_b)$  in this sample.
- The production of a  $D^{*\pm}$  in  $b\bar{b}$  events can arise from two different processes namely, through the cascade decay  $b \rightarrow c \rightarrow D^{*+}$  and from  $W$  decay  $b \rightarrow W \rightarrow D^{*-}$ . The effects of mixing in the  $B^0\bar{B}^0$  system must be taken into account for each. The dilution from these sources has been calculated in [8] in terms of a effective  $\chi$  parameter,  $\chi_{eff}$ . The dilution from mixing ( $\chi_{mix}$ ) and that from  $W$  production of  $D^{*\pm}$  ( $\chi_{D^*}$ ) have values :

$$\chi_{mix} = 0.152 (\pm 0.036)$$

$$\chi_{D^*} = 0.035 (\pm 0.035)$$

where the latter's error reflects the large uncertainty from the Monte Carlo estimate. The effective dilution parameter are expected to be :

$$\chi_{eff} = 0.176 (\pm 0.078)$$

The philosophy adopted here is to incorporate all such corrections into the  $(\epsilon_c, \epsilon_b)$  factors applied in equation (3). These are derived from Monte Carlo and are given in Table 4 together with their statistical and systematic errors. The values of  $\epsilon_b$  are larger than the  $\chi_{eff}$  value quoted above. This is due to the additional effect from the improvement in the thrust axis determination in the presence of a fast  $D^{*\pm}$ .

$\kappa$	$\langle Q_{opp}^{D^*} \rangle (K\pi)$	$\langle Q_{opp}^{D^*} \rangle (K\pi\pi\pi)$	$\langle Q_{opp}^{D^*} \rangle (K\pi\pi^0)$	Combined $\langle Q_{opp}^{D^*} \rangle$
0.3	$0.0667 \pm 0.0061$	$0.0693 \pm 0.0066$	$0.0664 \pm 0.0059$	$0.0674 \pm 0.0036$
0.4	$0.0673 \pm 0.0066$	$0.0681 \pm 0.0071$	$0.0679 \pm 0.0064$	$0.0678 \pm 0.0039$
0.5	$0.0675 \pm 0.0073$	$0.0665 \pm 0.0077$	$0.0691 \pm 0.0070$	$0.0678 \pm 0.0042$
0.7	$0.0671 \pm 0.0088$	$0.0623 \pm 0.0092$	$0.0704 \pm 0.0083$	$0.0669 \pm 0.0050$
0.9	$0.0660 \pm 0.0104$	$0.0579 \pm 0.0109$	$0.0706 \pm 0.0097$	$0.0653 \pm 0.0059$
1.0	$0.0653 \pm 0.0112$	$0.0558 \pm 0.0117$	$0.0704 \pm 0.0104$	$0.0643 \pm 0.0064$
1.2	$0.0638 \pm 0.0128$	$0.0521 \pm 0.0132$	$0.0694 \pm 0.0118$	$0.0624 \pm 0.0072$
1.5	$0.0617 \pm 0.0148$	$0.0482 \pm 0.0153$	$0.0672 \pm 0.0135$	$0.0597 \pm 0.0084$
2.0	$0.0591 \pm 0.0175$	$0.0455 \pm 0.0180$	$0.0628 \pm 0.0159$	$0.0565 \pm 0.0099$
$\infty$	$0.0530 \pm 0.0206$	$0.0379 \pm 0.0199$	$0.0587 \pm 0.0199$	$0.0506 \pm 0.0116$

Table 3: Hemisphere charges opposite a true  $D^{*\pm}$  after correcting for contributions from light quark and combinatoric events from the side-band of the selected modes.

$\kappa$	$\epsilon_c$	$\epsilon_b$
0.3	$-0.0005 \pm 0.0007$	$-0.0436 \pm 0.0195$
0.4	$-0.0022 \pm 0.0008$	$-0.0489 \pm 0.0218$
0.5	$-0.0029 \pm 0.0008$	$-0.0544 \pm 0.0243$
0.7	$-0.0061 \pm 0.0010$	$-0.0652 \pm 0.0290$
0.9	$-0.0092 \pm 0.0012$	$-0.0753 \pm 0.0334$
1.0	$-0.0100 \pm 0.0013$	$-0.0799 \pm 0.0354$
1.2	$-0.0110 \pm 0.0015$	$-0.0884 \pm 0.0391$
1.5	$-0.0130 \pm 0.0018$	$-0.0988 \pm 0.0435$
2.0	$-0.0189 \pm 0.0021$	$-0.1108 \pm 0.0487$
$\infty$	$-0.0256 \pm 0.0023$	$-0.1201 \pm 0.0145$

Table 4: Correction factors applied to  $\delta_c$  and  $\delta_b$  to take into account bias from the  $D^{*\pm}$  selection and the effective mixing in  $b\bar{b}$  events. The errors on  $\epsilon_c$  represent the statistical errors only, whereas those on  $\epsilon_b$  include a 100% systematic uncertainty from the Monte Carlo expectation of the dilution from  $b \rightarrow W \rightarrow D^{*-}$  decays.

### 2.3 Extraction of $\delta_c$

$\delta_c$  is extracted by solving equation (3) using combined values of  $\langle Q_{opp}^{D^*} \rangle$  from Table 3.  $\delta_b$  is also needed and is taken from the measurements made using the lifetime tag [9, 10] which are given later in Section 3. The extracted values of  $\delta_c$  from the combined  $D^{*\pm}$  sample are given in Table 5. The errors reflect the propagated statistical and systematic errors from equation (3)

$\kappa$	$\delta_c^{D^*}$	
0.3	0.1881	$\pm 0.0109$
0.4	0.1899	$\pm 0.0119$
0.5	0.1917	$\pm 0.0131$
0.7	0.1913	$\pm 0.0157$
0.9	0.1886	$\pm 0.0184$
1.0	0.1876	$\pm 0.0197$
1.2	0.1854	$\pm 0.0221$
1.5	0.1812	$\pm 0.0253$
2.0	0.1723	$\pm 0.0295$
$\infty$	0.1656	$\pm 0.0321$

Table 5: *Extracted values of  $\delta_c$  from the combined sample of  $D^{*\pm}$  events.*

although they are dominated by the statistical error from  $\langle Q_{opp} \rangle$  due to the small samples of selected  $D^{*\pm}$ .

## 3 A Measurement of $\delta_c$ Using a Lifetime Tag

The analysis is a modified form of that described in [9] and only improvements and modifications are summarised here. The quantity,  $\bar{\delta}$ , is measured in a series of increasingly pure  $b\bar{b}$  samples selected using the lifetime tag algorithm, QIPBTAG [11]. The value of  $\bar{\delta}$  for a pure sample of quarks of flavour  $f$  (ie.  $\bar{\delta}_f$ ) may be related directly to the charge separation for that flavour,  $\delta_f$ , by :

$$\begin{aligned}
 \bar{\delta}_f^2 &= \left(\sigma_{FB}^f\right)^2 - \left(\sigma_Q^f\right)^2 = -4\langle Q_F Q_B \rangle - \langle Q_{FB}^f \rangle^2 + \langle Q^f \rangle^2 \\
 &= \delta_f^2 - \underbrace{4\langle \mathcal{R}_f \mathcal{R}_{\bar{f}} \rangle - \langle Q_{FB}^f \rangle^2 + \langle Q^f \rangle^2}_{\text{Correction Terms} = C_f}
 \end{aligned}
 \tag{4}$$

Measurements of  $\bar{\delta}$  are shown in Figure 1 and make use of 1991  $\rightarrow$  1993 data. They have been corrected for the bias introduced by the lifetime tag and include both statistical and systematic errors as evaluated in [9, 10]. The sample flavour composition is varied using a cut on the lifetime tag hemisphere probabilities. The expected dependence on flavour composition is observed and may be understood by considering that  $\bar{\delta}$  can be written as :

$$\bar{\delta} = \sqrt{\sum_{f=u,d,\dots}^b \mathcal{P}_f \bar{\delta}_f^2}
 \tag{5}$$

where  $\mathcal{P}_f$  is the purity of flavour  $f$ . The flavour composition of events selected by the lifetime tag has several components; those flavours where the primary meson has a lifetime and those where it does not. Hence, the flavour purities are broken down into that for light quarks,  $\mathcal{P}_{uds}$ , and heavy flavours,  $\mathcal{P}_c$  and  $\mathcal{P}_b$ . It is important to note that light flavours are assumed to tag with equal efficiencies. This is known not to be exactly true, especially for severe lifetime tag

selections and so represents a source of systematic uncertainty in the interpretation of the light quark constraints.

Previously, a cubic fit to  $\bar{\delta}(\mathcal{P}_b)$  was used to extract  $\bar{\delta}_b$  from an estimate of the value of  $\bar{\delta}$  at the limit of 100%  $b$  purity. These are shown in Figure 1. This method is improved upon since the values of  $\mathcal{P}_{uds}$  and  $\mathcal{P}_c$  are known from [11]. They can be parameterised using polynomials and used to fit for  $\bar{\delta}_{uds}$ ,  $\bar{\delta}_c$  and  $\bar{\delta}_b$  individually. The parameterisations of  $\mathcal{P}_{uds}$  and  $\mathcal{P}_c$  as a function of  $\mathcal{P}_b$  are shown in Figure 2. The parameterisations are used in a “free fit” of  $\bar{\delta}_{uds}$ ,  $\bar{\delta}_c$  and  $\bar{\delta}_b$  as superimposed onto Figure 1. Errors from light and  $c\bar{c}$  quark purity parameterisations are propagated through to the values of  $\bar{\delta}$  which are used in the fit. This yields a conservative error estimate as it ignores correlations between the errors on  $\mathcal{P}_{uds}$ ,  $\mathcal{P}_c$  and  $\mathcal{P}_b$ .

The fitted values of  $\bar{\delta}_{uds}$ ,  $\bar{\delta}_c$  and  $\bar{\delta}_b$  are given in Table 6 where the latter are compared with the extrapolated values from the cubic fits used previously. The two methods of extracting  $\bar{\delta}_b$  are

$\kappa$	<i>Fitted</i> $\bar{\delta}_{uds}$	<i>Fitted</i> $\bar{\delta}_c$	<i>Fitted</i> $\bar{\delta}_b$	<i>Extrapolated</i> $\bar{\delta}_b$
0.3	0.2200 $\pm$ 0.0026	0.2131 $\pm$ 0.0095	0.1522 $\pm$ 0.0021	0.1510 $\pm$ 0.0033
0.4	0.2310 $\pm$ 0.0028	0.2113 $\pm$ 0.0108	0.1575 $\pm$ 0.0023	0.1565 $\pm$ 0.0036
0.5	0.2452 $\pm$ 0.0031	0.2109 $\pm$ 0.0125	0.1660 $\pm$ 0.0025	0.1655 $\pm$ 0.0040
0.7	0.2784 $\pm$ 0.0038	0.2123 $\pm$ 0.0170	0.1883 $\pm$ 0.0031	0.1882 $\pm$ 0.0049
0.9	0.3120 $\pm$ 0.0045	0.2142 $\pm$ 0.0219	0.2128 $\pm$ 0.0036	0.2134 $\pm$ 0.0058
1.0	0.3276 $\pm$ 0.0049	0.2149 $\pm$ 0.0247	0.2247 $\pm$ 0.0038	0.2259 $\pm$ 0.0063
1.2	0.3557 $\pm$ 0.0057	0.2157 $\pm$ 0.0307	0.2467 $\pm$ 0.0044	0.2483 $\pm$ 0.0071
1.5	0.3896 $\pm$ 0.0066	0.2142 $\pm$ 0.0389	0.2741 $\pm$ 0.0051	0.2764 $\pm$ 0.0081
2.0	0.4283 $\pm$ 0.0079	0.2078 $\pm$ 0.0519	0.3057 $\pm$ 0.0060	0.3088 $\pm$ 0.0095

Table 6: Results of the fit to  $\bar{\delta}_{uds}$ ,  $\bar{\delta}_c$  and  $\bar{\delta}_b$  and comparison with the extrapolated values of  $\bar{\delta}_b$  used previously.

seen to yield compatible results. The fit is seen to fail for  $\kappa = \infty$ . This is because of statistical fluctuations in the data which lead to a preference for :

$$\bar{\delta}_c = 0.0009 \pm 0.2630 \quad (6)$$

This results in a bias on the corresponding values for  $\bar{\delta}_{uds}$  and  $\bar{\delta}_b$  which yield the values :

$$\bar{\delta}_{uds} = 0.5153 \pm 0.0044 \quad (7)$$

$$\bar{\delta}_b = 0.3507 \pm 0.0044 \quad (8)$$

and alters the intercorrelation between the three values of  $\bar{\delta}$ . This is understood to be an artifact using the current statistics<sup>3</sup> in the free fit. This does not affect the extrapolated values of  $\bar{\delta}_b$  but means that the  $\bar{\delta}_c$  and  $\bar{\delta}_{uds}$  are not available for this  $\kappa$ .

The “correction terms” of equation (4) are extracted from Monte Carlo simulation. It is shown in [9, 10] that such corrections are small and relatively insensitive to fragmentation model parameters. The latter is difficult to check with high precision due to the limitations of Monte Carlo statistics and remains the dominant uncertainty of the method. Correction terms for  $u$ ,  $d$ ,  $s$  and  $c$  quarks are given in Table 7 in the context of simulated HVFLO3. The corrections assume the forward-backward asymmetries and  $\langle Q_f \rangle$  values inherent in the simulation. The former are based on a  $\sin^2\theta_W^{eff}$  value of 0.232 however uncertainties arising from use of these quantities are negligible. A further relative systematic uncertainty of 15% is assumed on the correction terms based upon that calculated for  $C_b$  in [10]. The extracted values of  $\delta_c$  are given in Table 8.

<sup>3</sup>Note that the  $Q_{FB}$  distribution at  $\kappa = \infty$  consists of three delta functions at charges of  $(-2, 0, +2)$  which leads to large statistical uncertainties than that found at lower  $\kappa$ .

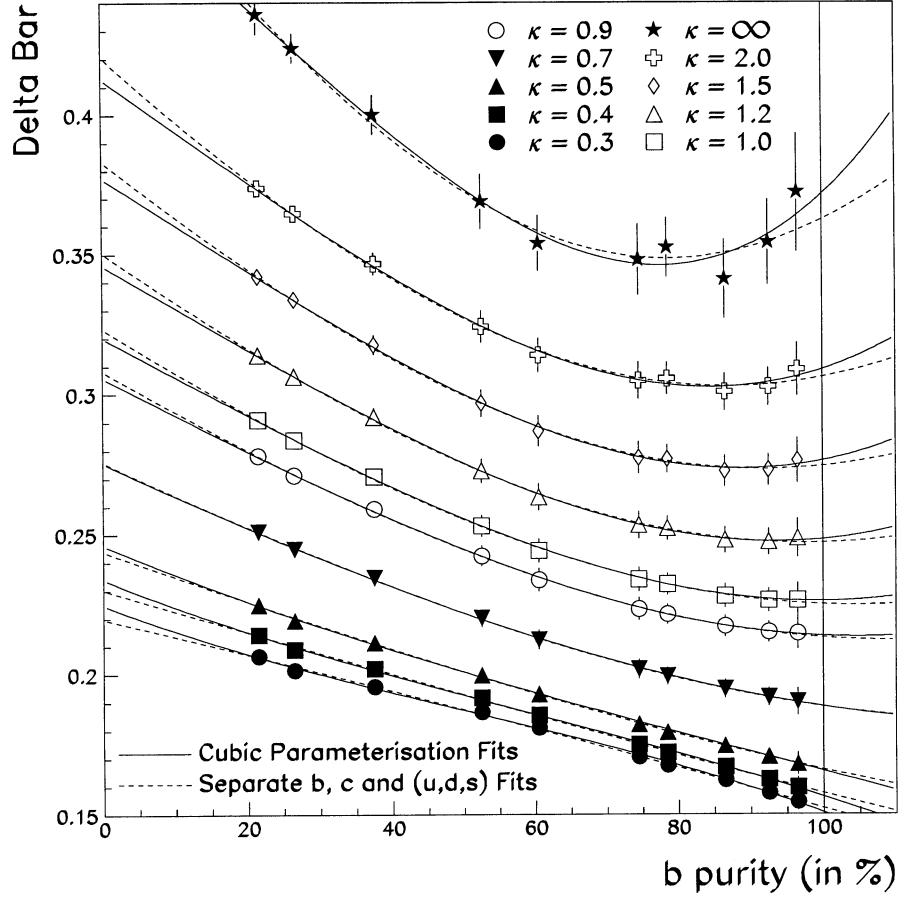


Figure 1: Values of  $\bar{\delta}$  in data as a function of  $b$  purity. Results are shown for a variety of  $\kappa$  values with both cubic and free fits superimposed.

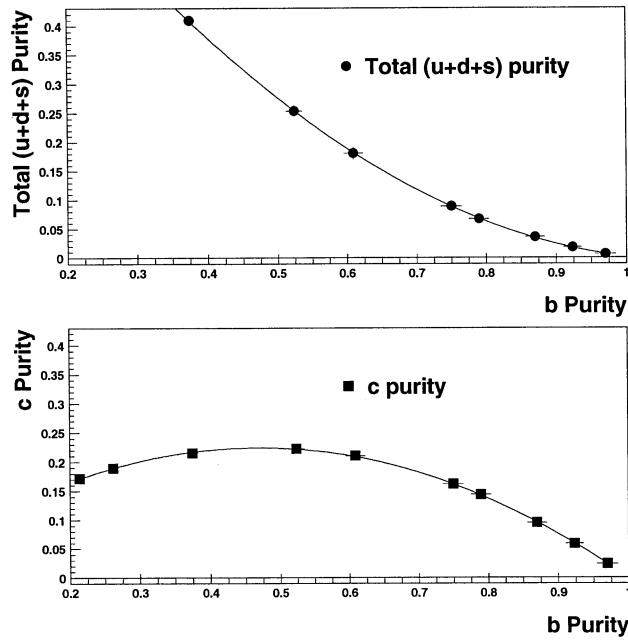


Figure 2: Fitted parameterisations to light ( $u, d, s$ ) and  $c$  quark purities as a function of the  $b$  purity,  $\mathcal{P}_b$ .

$\kappa$	$u$ Corr.		$d$ Corr.		$s$ Corr.		$c$ Corr.		$b$ Corr.	
0.3	0.018	$\pm 0.003$	0.014	$\pm 0.002$	0.015	$\pm 0.002$	0.012	$\pm 0.002$	0.011	$\pm 0.001$
0.4	0.016	$\pm 0.002$	0.011	$\pm 0.002$	0.012	$\pm 0.002$	0.009	$\pm 0.001$	0.009	$\pm 0.001$
0.5	0.015	$\pm 0.002$	0.009	$\pm 0.002$	0.010	$\pm 0.002$	0.007	$\pm 0.002$	0.008	$\pm 0.001$
0.7	0.015	$\pm 0.002$	0.006	$\pm 0.002$	0.009	$\pm 0.002$	0.004	$\pm 0.002$	0.008	$\pm 0.001$
0.9	0.018	$\pm 0.004$	0.005	$\pm 0.002$	0.009	$\pm 0.002$	0.003	$\pm 0.001$	0.008	$\pm 0.001$
1.0	0.019	$\pm 0.004$	0.005	$\pm 0.002$	0.010	$\pm 0.002$	0.002	$\pm 0.001$	0.008	$\pm 0.001$
1.2	0.022	$\pm 0.004$	0.005	$\pm 0.002$	0.011	$\pm 0.003$	0.002	$\pm 0.001$	0.009	$\pm 0.001$
1.5	0.026	$\pm 0.005$	0.005	$\pm 0.003$	0.014	$\pm 0.004$	0.001	$\pm 0.002$	0.011	$\pm 0.002$
2.0	0.032	$\pm 0.006$	0.006	$\pm 0.003$	0.017	$\pm 0.004$	0.001	$\pm 0.003$	0.014	$\pm 0.003$
$\infty$	0.049	$\pm 0.011$	0.010	$\pm 0.008$	0.026	$\pm 0.009$	0.000	$\pm 0.007$	0.018	$\pm 0.010$

Table 7: Correlation corrections for  $u$ ,  $d$ ,  $s$  and  $c$  quarks for various  $\kappa$  values. The combined statistical and systematic error is given.

## 4 Combined Fits of $D^{*\pm}$ and Lifetime Tag Measurements

Given the relatively low precision of the individual  $D^{*\pm}$  and lifetime tag measurements of  $\delta_c$ , it is of interest to combine them. The two measurements of  $\delta_c$  presented here are complementary in that the  $D^{*\pm}$  analysis indicates both the sign and magnitude of  $\delta_c$  whereas the lifetime measurements only give the absolute<sup>4</sup> value. This task of combining the two sets of values is complicated by correlations arising from several sources :

- The measurements at different  $\kappa$  values are intercorrelated.
- The lifetime tagged values of  $\delta_c$  and  $\delta_b$  are correlated through the simultaneous fit to the measured  $\bar{\delta}$
- The  $D^{*\pm}$  method of measuring  $\delta_c$  makes use of the lifetime tagged values of  $\delta_b$ . This introduces a significant correlation between the  $D^{*\pm}$  and lifetime tag measurements of  $\delta_c$ .
- The small overlap between the event samples for the lifetime tagged and  $D^{*\pm}$  measurements further correlates the two sets of measurements.

Hence, a  $\chi^2$  fit is performed using correlation matrices derived from the two methods. These matrices are obtained from :

- *Correlations between  $\kappa$  values* - These are obtained from the data in both the  $D^{*\pm}$  and lifetime tagged measurements.
- *Correlations between  $\delta_c$  and  $\delta_b$  from the lifetime tag* - These are obtained from data using the fits described in Section 3 and shown in Figure 1.
- *Correlations between  $\delta_c$  from  $D^{*\pm}$  and  $\delta_c$  and  $\delta_b$  from the lifetime tag* - There is a small statistical intercorrelation between the two sets of measurements which arise from the small overlap in the data samples. The effect of this is conservatively estimated by studying how many of the selected  $D^{*\pm}$  events are present in the “heavy flavour” regime<sup>5</sup> of the data. Running the lifetime tag analysis on the  $D^{*\pm}$  sample used in Section 2 indicates that they are selected with an efficiency between 33 and 45%. Taking into account the total sample

<sup>4</sup>The analogous case for  $\delta_b$  is when the lepton signed hemisphere charge may be used to infer the sign of the lifetime tag measurements.

<sup>5</sup>This corresponds to the region of Figure 1 where the  $c\bar{c}$  and  $b\bar{b}$  contributions dominate, assumed to when the  $b$  purity is above  $\sim 60\%$ .



$\kappa$	$\delta_c$ from $\bar{\delta}$
0.3	0.183 $\pm$ 0.012
0.4	0.188 $\pm$ 0.013
0.5	0.193 $\pm$ 0.015
0.7	0.202 $\pm$ 0.020
0.9	0.207 $\pm$ 0.025
1.0	0.209 $\pm$ 0.028
1.2	0.211 $\pm$ 0.034
1.5	0.211 $\pm$ 0.043
2.0	0.205 $\pm$ 0.056

Table 8: Measured values of  $\delta_c$  from the free fit to  $\bar{\delta}$ . Errors represent total statistical and systematic uncertainties.

sizes in this region and assuming conservative estimates of the tagging efficiencies results in a 10 ( $\pm$ 3) % correlation between the data used in the two methods. This ignores the fact that the  $D^{*\pm}$  method only makes of one hemisphere per event.

- *Correlations between the  $(\epsilon_c, \epsilon_b)$  factors at different  $\kappa$  values* - The correlation between these factors is, like the factors themselves, assumed from Monte Carlo.

In the case of the lifetime tag measurements, the correlation matrices for  $\delta_c$  and  $\delta_b$ , at different  $\kappa$  values, are the same since they are fitted to a single quantity,  $\bar{\delta}$ . In addition, the correlation between  $\delta_c$  and  $\delta_b$  in the lifetime tag analysis remains approximately constant with  $\kappa$  at a value of -0.8. These considerations help to simplify the fitting procedure considerably. The  $(\epsilon_c, \epsilon_b)$  factors and  $c\bar{c}$  fraction ( $f_c$ ) are allowed to float in the fit within their combined statistical and systematic errors. The results of the combined fit are given in Table 9. The values for  $(\epsilon_c, \epsilon_b)$  and  $f_c$  after the fit are almost unchanged and remain well within their expected uncertainties.

## 5 Results and Comparisons with Model Expectations

Results of the combined fit of  $\delta_c$  in data are compared with Monte Carlo expectations from HVFL03 in Figure 3. From this it is clear that there is a strong,  $\kappa$  dependent discrepancy between the two. The studies of how the various charm branching fractions affect the values of  $\delta_c$  are presented in [6]. Using the 1992 PDG values for the inclusive rates of  $D^0$  or  $D^+ \rightarrow K + X$  is seen to increase the absolute value of  $\delta_c$  for all  $\kappa$ . These corrected expectations for  $\delta_c$  are also shown in Figure 3 and give close agreement with that found in data.

The fitted values of  $\bar{\delta}_{uds}$  may also be compared with model expectations, however their interpretation is less simple than that of single quark flavours. It may be written as :

$$\bar{\delta}_{uds}^{-2} = \frac{\mathcal{P}_u}{\mathcal{P}_u + \mathcal{P}_d + \mathcal{P}_s} \bar{\delta}_u^{-2} + \frac{\mathcal{P}_d}{\mathcal{P}_d + \mathcal{P}_d + \mathcal{P}_s} \bar{\delta}_u^{-2} + \frac{\mathcal{P}_s}{\mathcal{P}_s + \mathcal{P}_d + \mathcal{P}_s} \bar{\delta}_u^{-2} \quad (9)$$

The assumption that the tagging efficiencies of light quarks are equal means that :

$$\frac{\mathcal{P}_u}{\mathcal{P}_u + \mathcal{P}_d + \mathcal{P}_s} = 0.2804 \text{ and } \frac{\mathcal{P}_d}{\mathcal{P}_u + \mathcal{P}_d + \mathcal{P}_s} = \frac{\mathcal{P}_s}{\mathcal{P}_u + \mathcal{P}_d + \mathcal{P}_s} = 0.3598 \quad (10)$$

Under this assumption,  $\bar{\delta}_u$ ,  $\bar{\delta}_d$  and  $\bar{\delta}_s$  values from simulated Monte Carlo may be used to calculate  $\bar{\delta}_{uds}$  and compared with that found in data. This is shown in Figure 4 with the values given in Table 10. A systematic uncertainty due to assumption (10) is shown for the Monte Carlo

$\kappa$	$\delta_c$	$\delta_b$
0.3	$0.1854 \pm 0.0087$	$-0.1124 \pm 0.0038$
0.4	$0.1885 \pm 0.0099$	$-0.1263 \pm 0.0039$
0.5	$0.1913 \pm 0.0109$	$-0.1407 \pm 0.0039$
0.7	$0.1936 \pm 0.0136$	$-0.1688 \pm 0.0046$
0.9	$0.1934 \pm 0.0160$	$-0.1947 \pm 0.0056$
1.0	$0.1931 \pm 0.0173$	$-0.2070 \pm 0.0060$
1.2	$0.1918 \pm 0.0196$	$-0.2293 \pm 0.0066$
1.5	$0.1881 \pm 0.0228$	$-0.2567 \pm 0.0072$
2.0	$0.1791 \pm 0.0271$	$-0.2868 \pm 0.0108$

Table 9: Results of the combined fit for  $\delta_c$  using the  $D^{*\pm}$  and lifetime tag methods. The values of  $\delta_b$  used in the fit are also given.

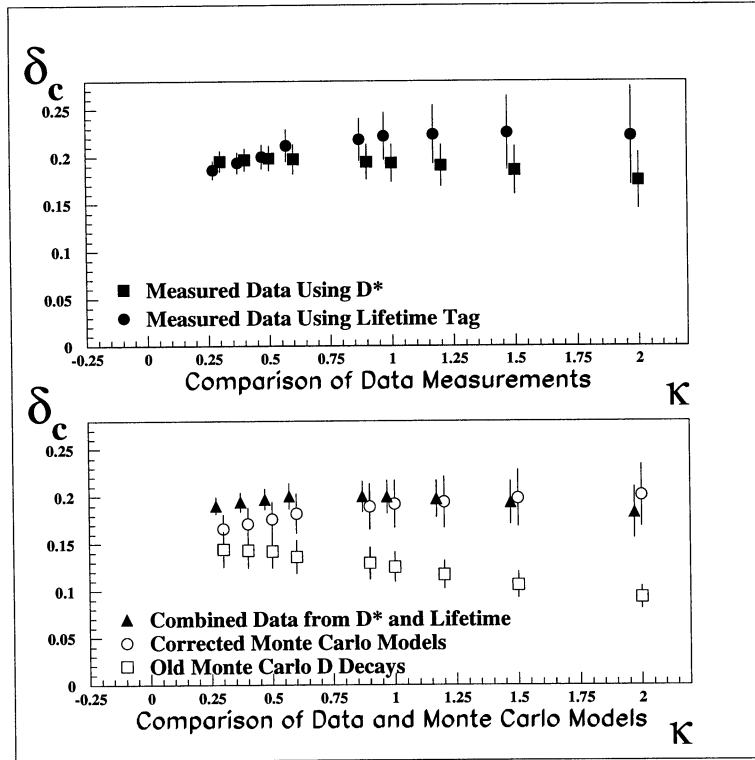


Figure 3: Comparisons of (a) the lifetime tag and  $D^{*\pm}$  measurements of  $\delta_c$  and (b) the combined  $\delta_c$  measurement in data with that expected from Monte Carlo simulation using different charm branching ratios.

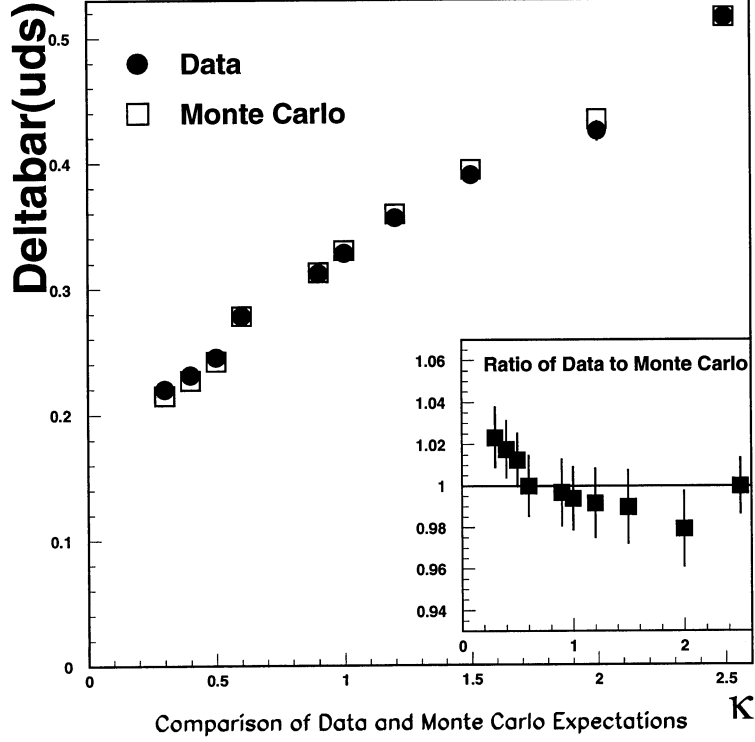


Figure 4: Comparison of the measured  $\bar{\delta}_{uds}$  in data with that expected from Monte Carlo. The ratio is shown in the insert.

$\kappa$	Measured $\bar{\delta}_{uds}$	Monte Carlo $\bar{\delta}_{uds}$
0.3	0.220 $\pm$ 0.003	0.215 $\pm$ 0.001
0.4	0.231 $\pm$ 0.003	0.227 $\pm$ 0.001
0.5	0.245 $\pm$ 0.003	0.242 $\pm$ 0.001
0.7	0.278 $\pm$ 0.004	0.278 $\pm$ 0.001
0.9	0.312 $\pm$ 0.005	0.313 $\pm$ 0.001
1.0	0.328 $\pm$ 0.005	0.330 $\pm$ 0.001
1.2	0.356 $\pm$ 0.006	0.359 $\pm$ 0.001
1.5	0.390 $\pm$ 0.007	0.394 $\pm$ 0.001
2.0	0.428 $\pm$ 0.008	0.434 $\pm$ 0.001
$\infty$	0.516 $\pm$ 0.007	0.516 $\pm$ 0.001

Table 10: Measured values of  $\bar{\delta}_{uds}$  in data compared to that expected from Monte Carlo. The errors on Monte Carlo come from statistics and an estimate of the difference in the  $u$ ,  $d$  and  $s$  purities when selected using the lifetime tag.

values in Figure 4. This is estimated from the differences in the light quark tagging efficiencies observed in Monte Carlo. Data and Monte Carlo are seen to be in agreement over a wide range of the weighting parameter,  $\kappa$ .

## 6 Conclusions

$\delta_c$  is extracted from two samples of events. One tagged by the presence of a fast  $D^{*\pm}$  and the other using a lifetime tag. The results are consistent with each other and achieve a combined accuracy of 8% at  $\kappa = 1$ . The measured values and  $\kappa$  dependence indicate that charm branching fractions, presently used inside the HVFL generator, do not reproduce a  $\delta_c$  which agrees with that found in data. However, more recent branching fraction measurements show that inclusive rates can improve the situation.

The combined charge separations for light quarks, after subtraction of  $\bar{\delta}_c$  and  $\bar{\delta}_b$ , are in agreement with model expectations and offer the possibility of using them in conjunction with further measurements to extract the light quark separations directly. The overall agreement between data and simulation for the value of  $\delta$  with 5 flavours is maintained at a comparable accuracy (less than 1%) when only ( $u, d, s$ ) flavours are considered.

The impact of  $\delta_c$  and  $\delta_b$  uncertainties on the systematic error of  $\sin^2\theta_W^{eff}$  in the  $Q_{FB}$  analysis are estimated<sup>6</sup> to be  $\Delta\sin^2\theta_W^{eff} = 0.0005$  and  $0.0003$  respectively. Their contribution to the total error is small compared to that due to light quarks.

## 7 Acknowledgements

The authors are indebted to C. Boyer, P. Colas and D. Pallin for providing well studied samples of  $D^{*\pm}$  and background events and to A. Blondel and R. StDenis for their ideas on extending the lifetime tag analysis to the charm sector.

## A Appendix - Measurements Using a Thrust Axis Made from Charged Tracks Only

The results of this analysis are presented here using the charged track objects to form the thrust axis. This has relatively little effect and is only included so as to maintain consistency between the combined hadronic asymmetry measurement [1, 2] and that of the  $A_{FB}^b$  analysis [3]. The following Tables 11 to 14 given here are analogous to those of Tables 2 to 5 in Section 2.

The lifetime tag analysis was also repeated using charged tracks only to derive the thrust axis direction. The results of this analysis are given in Table 15, showing the  $\delta_c$  and  $\delta_b$  results obtained. The results of the combined fit to  $\delta_c$  from  $D^{*\pm}$  and lifetime tag methods for the charged track thrust axis are given in Table 16. Within the given precision, these are entirely consistent with that found for the ENFLW axis.

## References

- [1] The ALEPH Collaboration, D. Decamp et al, *Physics Letters*, **B 259** 377, (1991).
- [2] A. Blondel et al, *Determination of  $\sin^2\theta_W^{eff}$  from the Hadronic Charge Asymmetry*, ALEPH Note 93-044, PHYSIC 93-035, March 1993.
- [3] The ALEPH Collaboration, D. Buskulic et al, *Physics Letters*, **B 335** 99, (1994).

---

<sup>6</sup>Using HVFL03 at  $\kappa = 1.0$  and currently ignoring the correlations between  $\delta_c$  and  $\delta_b$ .

$\kappa$	$\langle Q_{opp} \rangle(K\pi)$	$\langle Q_{opp} \rangle(K\pi\pi\pi)$	$\langle Q_{opp} \rangle(K\pi\pi^0)$
0.3	$0.0677 \pm 0.0055$	$0.0367 \pm 0.0032$	$0.0446 \pm 0.0034$
0.4	$0.0679 \pm 0.0060$	$0.0361 \pm 0.0035$	$0.0452 \pm 0.0037$
0.5	$0.0677 \pm 0.0066$	$0.0352 \pm 0.0039$	$0.0456 \pm 0.0041$
0.7	$0.0666 \pm 0.0081$	$0.0332 \pm 0.0047$	$0.0459 \pm 0.0049$
0.9	$0.0649 \pm 0.0098$	$0.0310 \pm 0.0056$	$0.0455 \pm 0.0058$
1.0	$0.0639 \pm 0.0106$	$0.0300 \pm 0.0060$	$0.0451 \pm 0.0062$
1.2	$0.0619 \pm 0.0121$	$0.0282 \pm 0.0069$	$0.0440 \pm 0.0071$
1.5	$0.0589 \pm 0.0141$	$0.0263 \pm 0.0080$	$0.0418 \pm 0.0082$
2.0	$0.0549 \pm 0.0167$	$0.0251 \pm 0.0094$	$0.0377 \pm 0.0097$
$\infty$	$0.0479 \pm 0.0197$	$0.0213 \pm 0.0102$	$0.0297 \pm 0.0122$

Table 11: Measured Values of  $\langle Q_{opp} \rangle$  for the three selected  $D^{*\pm}$  modes using the thrust axis calculated from charged tracks only.

$\kappa$	$\langle Q_{opp}^{D^*} \rangle(K\pi)$	$\langle Q_{opp}^{D^*} \rangle(K\pi\pi\pi)$	$\langle Q_{opp}^{D^*} \rangle(K\pi\pi^0)$	Combined $\langle Q_{opp}^{D^*} \rangle$
0.3	$0.0707 \pm 0.0062$	$0.0670 \pm 0.0065$	$0.0708 \pm 0.0060$	$0.0696 \pm 0.0036$
0.4	$0.0709 \pm 0.0066$	$0.0663 \pm 0.0071$	$0.0721 \pm 0.0065$	$0.0699 \pm 0.0039$
0.5	$0.0707 \pm 0.0073$	$0.0651 \pm 0.0077$	$0.0732 \pm 0.0071$	$0.0699 \pm 0.0043$
0.7	$0.0696 \pm 0.0088$	$0.0621 \pm 0.0092$	$0.0744 \pm 0.0085$	$0.0690 \pm 0.0051$
0.9	$0.0678 \pm 0.0104$	$0.0588 \pm 0.0109$	$0.0746 \pm 0.0100$	$0.0675 \pm 0.0060$
1.0	$0.0669 \pm 0.0113$	$0.0572 \pm 0.0117$	$0.0743 \pm 0.0107$	$0.0666 \pm 0.0065$
1.2	$0.0648 \pm 0.0128$	$0.0544 \pm 0.0133$	$0.0731 \pm 0.0121$	$0.0646 \pm 0.0073$
1.5	$0.0617 \pm 0.0149$	$0.0515 \pm 0.0154$	$0.0705 \pm 0.0139$	$0.0618 \pm 0.0085$
2.0	$0.0576 \pm 0.0175$	$0.0501 \pm 0.0181$	$0.0651 \pm 0.0163$	$0.0580 \pm 0.0100$
$\infty$	$0.0523 \pm 0.0206$	$0.0452 \pm 0.0190$	$0.0549 \pm 0.0204$	$0.0511 \pm 0.0115$

Table 12: Hemisphere charges opposite a true  $D^{*\pm}$  after correcting for contributions from light quark and combinatoric events from the side-band of the selected modes using the thrust axis calculated from charged tracks only.

$\kappa$	$\epsilon_c$	$\epsilon_b$
0.3	$+0.0011 \pm 0.0007$	$-0.0433 \pm 0.0195$
0.4	$-0.0008 \pm 0.0007$	$-0.0486 \pm 0.0218$
0.5	$-0.0018 \pm 0.0008$	$-0.0540 \pm 0.0243$
0.7	$-0.0054 \pm 0.0010$	$-0.0648 \pm 0.0290$
0.9	$-0.0089 \pm 0.0012$	$-0.0748 \pm 0.0334$
1.0	$-0.0099 \pm 0.0013$	$-0.0794 \pm 0.0354$
1.2	$-0.0113 \pm 0.0014$	$-0.0879 \pm 0.0391$
1.5	$-0.0137 \pm 0.0017$	$-0.0982 \pm 0.0435$
2.0	$-0.0201 \pm 0.0020$	$-0.1102 \pm 0.0486$
$\infty$	$-0.0256 \pm 0.0023$	$-0.1201 \pm 0.0492$

Table 13: Correction factors applied to  $\delta_c$  and  $\delta_b$  to take into account bias from the  $D^{*\pm}$  selection and the effective mixing in  $b\bar{b}$  events. These corrections are calculated using the thrust axis calculated from charged tracks only. The errors on  $\epsilon_c$  represent the statistical errors only, whereas those on  $\epsilon_b$  include a 100% systematic uncertainty from the Monte Carlo expectation of the dilution from  $b \rightarrow W \rightarrow D^{*-}$  decays.

$\kappa$	$\delta_c^{D^*}$
0.3	0.1954 $\pm$ 0.0110
0.4	0.1969 $\pm$ 0.0120
0.5	0.1985 $\pm$ 0.0132
0.7	0.1976 $\pm$ 0.0158
0.9	0.1946 $\pm$ 0.0186
1.0	0.1934 $\pm$ 0.0199
1.2	0.1907 $\pm$ 0.0223
1.5	0.1856 $\pm$ 0.0255
2.0	0.1747 $\pm$ 0.0297
$\infty$	0.1655 $\pm$ 0.0342

Table 14: *Extracted values of  $\delta_c$  from the combined sample of  $D^{*\pm}$  events using the thrust axis calculated from charged tracks only.*

$\kappa$	$\delta_c$ from $\bar{\delta}$	$\delta_b$ from $\bar{\delta}$
0.3	0.186 $\pm$ 0.012	0.1118 $\pm$ 0.0042
0.4	0.194 $\pm$ 0.013	0.1265 $\pm$ 0.0042
0.5	0.200 $\pm$ 0.015	0.1416 $\pm$ 0.0044
0.7	0.212 $\pm$ 0.020	0.1707 $\pm$ 0.0051
0.9	0.218 $\pm$ 0.025	0.1977 $\pm$ 0.0060
1.0	0.222 $\pm$ 0.028	0.2102 $\pm$ 0.0065
1.2	0.223 $\pm$ 0.034	0.2326 $\pm$ 0.0074
1.5	0.225 $\pm$ 0.043	0.2598 $\pm$ 0.0087
2.0	0.222 $\pm$ 0.056	0.2907 $\pm$ 0.0106

Table 15: *Measured values of  $\delta_c$  and  $\delta_b$  from the free fit to  $\bar{\delta}$  using charged tracks only to determine the thrust axis. Errors represent total statistical and systematic uncertainties.*

$\kappa$	$\delta_c$	$\delta_b$
0.3	0.1903 $\pm$ 0.0089	-0.1130 $\pm$ 0.0039
0.4	0.1939 $\pm$ 0.0100	-0.1265 $\pm$ 0.0040
0.5	0.1970 $\pm$ 0.0111	-0.1409 $\pm$ 0.0040
0.7	0.2002 $\pm$ 0.0137	-0.1681 $\pm$ 0.0046
0.9	0.1996 $\pm$ 0.0162	-0.1937 $\pm$ 0.0057
1.0	0.1995 $\pm$ 0.0174	-0.2055 $\pm$ 0.0061
1.2	0.1974 $\pm$ 0.0197	-0.2276 $\pm$ 0.0066
1.5	0.1933 $\pm$ 0.0229	-0.2542 $\pm$ 0.0072
2.0	0.1829 $\pm$ 0.0273	-0.2825 $\pm$ 0.0109

Table 16: *Results of the combined fit for  $\delta_c$  using the  $D^{*\pm}$  and lifetime tag methods using charged tracks only to define the thrust axis of the event. The values of  $\delta_b$  used in the fit are also given.*

- [4] The ALEPH Collaboration, D. Decamp et al, *Physics Letters*, **B 284** 177-190, (1992).
- [5] T. Sjöstrand, *Computer Physics Commun.* **39** 347, (1986).  
T. Sjöstrand and M. Bengtsson, *Computer Physics Commun.* **43** 367, (1987).
- [6] P. Perrodo, *On Charm Charge Separation*, ALEPH Note 94-066, PHYSIC 94-058, May 1994.
- [7] C. Boyer et al, *The Forward-backward Asymmetry for Charm Quarks at the Z Pole*, ALEPH 94-089, PHYSIC 94-077, June 1994.
- [8] The ALEPH Collaboration, *The Forward-Backward Asymmetry for Charm Quarks at the Z Pole*, Paper Draft I, (To be submitted to Physics Letters B), January 1995.
- [9] A. Halley and P. Colrain, *A Measurement of the b Quark Hemisphere Charge Using a Lifetime-tag in the 1992 Data*, ALEPH Note 93-161, PHYSIC 93-138, October 1993.
- [10] A. Halley and P. Colrain, *Addendum to the Measurement of the b Quark Hemisphere Charge Using a Lifetime-Tag*, ALEPH Note 93-172, PHYSIC 93-147, November 1993.
- [11] The ALEPH Collaboration, D. Decamp et al, *Physics Letters*, **B 313** 535, (1993).